

Modulation effect in the differential rate for Supersymmetric Dark Matter detection.

J. D. VERGADOS

Theoretical Physics Section, University of Ioannina, GR-45110, Greece.

Abstract

The modulation effect in the direct detection of supersymmetric Cold Dark Matter (CDM) particles is investigated. It is shown that, while normally the modulation effect in the total event rate is small, $\leq 5\%$, in some special cases it becomes much larger. It also becomes more pronounced in the differential event rate. It may thus be exploited to discriminate against background.

1. INTRODUCTION

In this work we will study the differential modulation effect of the event rate for detecting supersymmetric dark matter, i.e. its variation with respect to the energy transferred to the nucleus, due to the Earth's motion.

There is now ample evidence that most of the matter of the Universe is non luminous, i.e. dark [1] and is composed of two components. One is the Hot Dark Matter (HDM) component consisting of particles which were relativistic at freeze out, while the other is the Cold Dark Matter (CDM) composed of particles which were non relativistic. There are many arguments supporting the fact that the CDM is at least 60% [2]. There are two interesting cold dark matter candidates: i) Massive Compact Halo Objects (MACHO's) and ii) Exotic Weakly Interacting Massive Particles (WIMP's). Since the MACHO's cannot exceed 40% of the CDM component [1, 3], there is room for an exotic candidate. The most natural one is associated with supersymmetry, i.e. the lightest supersymmetric particle (LSP).

The most interesting possibility to directly detect the LSP [1, 4] is via the recoil of a nucleus (A, Z) in the process:

$$\chi + (A, Z) \rightarrow \chi + (A, Z)^* \quad (1)$$

(χ denotes the LSP). In the above process only the elastic channel is open since the energy of the LSP is too low to excite the nucleus. In computing the event rate for the above process one proceeds with the following steps:

- 1) Write down the effective Lagrangian at the elementary particle (quark) level in the framework of supersymmetry as described in Refs. [1, 4].
- 2) Go from the quark to the nucleon level using an appropriate quark model for the nucleon. Special attention must be paid to the scalar couplings, which dominate the coherent part of the cross section and the isoscalar axial current, which strongly depend on the assumed quark model [4, 6].
- 3) Compute the relevant nuclear matrix elements [5, 7, 8, 9, 10] using as reliable as possible many body nuclear wave functions.
- 4) Calculate the modulation of the event rate due to the Earth's revolution around the sun [5, 11].

There are many popular targets [12, 13, 14] for LSP detection as e.g. ^{19}F , ^{23}Na , ^{27}Al , ^{29}Si , ^{40}Ca , $^{73,74}Ge$, ^{127}I , ^{207}Pb , etc.

In a previous paper [5] we computed the modulation effect h , i.e. the oscillation amplitude of the total event rate (see below for its precise definition), by convoluting with the LSP velocity distribution the event rate, which, among other things, depends upon the relative velocity of the LSP with respect to the Earth. Assuming a Maxwell Boltzmann distribution [1] of velocities for LSP, we found that h cannot exceed the value of 5% which corresponds to small momentum transfer. The actual value of h is quite a bit smaller especially for heavy nuclei and relatively heavy LSP ($m_\chi \geq 50\text{GeV}$). We showed that, in some cases, the quantity h may become negative suggesting cancellations between the bins that correspond to small and those which correspond to relatively large energy transfers. It is, thus, possible that in some energy bins the modulation effect can be larger than the the value of h quoted above.

The event rate depends on many parameters [4], since there exist many contributions to the above process. The most dominant appears to be the coherent contribution, which arises out of the scalar coupling originating from Higgs exchange or squark exchange if there exists mixing between the L and R squark varieties. It can also arise from the time component of the vector current originating from s-quark and Z-exchange. The latter is favored from the point of view of the couplings but it is suppressed kinematically by factors of $\beta^2 \sim 10^{-6}$ owing to the fact that the LSP is a Majorana particle. Due to its different dependence on the LSP velocity, it yields a higher modulation effect. In addition to the coherent part, especially for light targets, when the target spin is non zero, one must include the axial current (spin matrix element of the nucleus).

Our main purpose is to calculate the convoluted differential modulation effect H , i.e. the ratio of the part of the differential event rate which depends on the position of the Earth divided by that which does not (for its definition see below). If one considers each of the above mechanisms separately, H depends only on the LSP mass and the size of the nucleus. Knowledge of H may not be adequate, however, since one needs to know its value in the energy transfer regime where the event rate is the largest and hopefully measurable. One might also need the relative differential event rate, i.e. the ratio of the differential rate to the total rate. If one considers the above three mechanisms separately, the relative differential event rate is independent of the SUSY parameters or the structure of the nucleon. It depends on the nuclear structure only mildly through the form factors. So one can make quite accurate predictions which depend only on the nuclear size, the mass of the LSP and the low energy cutoff imposed by the detector.

2. EXPRESSIONS FOR THE RATE

As we have mentioned in the introduction we only need calculate the fraction of the differential rate divided by the total rate which is independent of the parameters of supersymmetry. Thus we are not going to elaborate here further on these, but refer the reader to the literature [4, 5, 15, 16]. For completeness we only give here expressions describing the effective Lagrangian obtained in first order via Higgs exchange, s-quark exchange and Z-exchange. We will use a formalism which is

familiar from the theory of weak interactions, i.e.

$$L_{eff} = -\frac{G_F}{\sqrt{2}} \{ (\bar{\chi}_1 \gamma^\lambda \gamma_5 \chi_1) J_\lambda + (\bar{\chi}_1 \chi_1) J \} \quad (2)$$

where

$$J_\lambda = \bar{N} \gamma_\lambda (f_V^0 + f_V^1 \tau_3 + f_A^0 \gamma_5 + f_A^1 \gamma_5 \tau_3) N \quad (3)$$

and

$$J = \bar{N} (f_s^0 + f_s^1 \tau_3) N \quad (4)$$

We have neglected the uninteresting pseudoscalar and tensor currents. Note that, due to the Majorana nature of the LSP, $\bar{\chi}_1 \gamma^\lambda \chi_1 = 0$ (identically). The parameters $f_V^0, f_V^1, f_A^0, f_A^1, f_S^0, f_S^1$ depend on the SUSY model employed. In SUSY models derived from minimal SUGRA the allowed parameter space is characterized at the GUT scale by five parameters, two universal mass parameters, one for the scalars, m_0 , and one for the gauginos, $m_{1/2}$, as well as the parameters $\tan\beta$, one of A_0 , or m_t^{pole} and the sign of μ [17]. Deviations from universality at the GUT scale have also been considered and found useful [18]. We will not elaborate further on this point since the above parameters involving universal masses have already been computed in some models [4, 19] and effects resulting from deviations from universality will be published elsewhere [20] (see also Arnowitt *et al* in Ref. [18]).

The invariant amplitude in the case of non-relativistic LSP can be cast in the form [4]

$$\begin{aligned} |\mathcal{M}|^2 &= \frac{E_f E_i - m_x^2 + \mathbf{p}_i \cdot \mathbf{p}_f}{m_x^2} |J_0|^2 + |\mathbf{J}|^2 + |J|^2 \\ &\simeq \beta^2 |J_0|^2 + |\mathbf{J}|^2 + |J|^2 \end{aligned} \quad (5)$$

where m_x is the LSP mass, $|J_0|$ and $|\mathbf{J}|$ indicate the matrix elements of the time and space components of the current J_λ of Eq. (3), respectively, and J represents the matrix element of the scalar current J of Eq. (4). Notice that $|J_0|^2$ is multiplied by β^2 (the suppression due to the Majorana nature of LSP mentioned above). It is straightforward to show that

$$|J_0|^2 = A^2 |F(\mathbf{q}^2)|^2 \left(f_V^0 - f_V^1 \frac{A - 2Z}{A} \right)^2 \quad (6)$$

$$J^2 = A^2 |F(\mathbf{q}^2)|^2 \left(f_S^0 - f_S^1 \frac{A - 2Z}{A} \right)^2 \quad (7)$$

$$|\mathbf{J}|^2 = \frac{1}{2J_i + 1} |\langle J_i | [f_A^0 \Omega_0(\mathbf{q}) + f_A^1 \Omega_1(\mathbf{q})] | J_i \rangle|^2 \quad (8)$$

with $F(\mathbf{q}^2)$ the nuclear form factor and

$$\Omega_0(\mathbf{q}) = \sum_{j=1}^A \sigma(j) e^{-i\mathbf{q} \cdot \mathbf{x}_j}, \quad \Omega_1(\mathbf{q}) = \sum_{j=1}^A \sigma(j) \tau_3(j) e^{-i\mathbf{q} \cdot \mathbf{x}_j} \quad (9)$$

where $\sigma(j)$, $\tau_3(j)$, \mathbf{x}_j are the spin, third component of isospin ($\tau_3|p\rangle = |p\rangle$) and coordinate of the j -th nucleon and \mathbf{q} is the momentum transferred to the nucleus.

The differential cross section in the laboratory frame takes the form [4]

$$\frac{d\sigma}{d\Omega} = \frac{\sigma_0}{\pi} \left(\frac{m_x}{m_N} \right)^2 \frac{1}{(1+\eta)^2} \xi \{ \beta^2 |J_0|^2 [1 - \frac{2\eta+1}{(1+\eta)^2} \xi^2] + |\mathbf{J}|^2 + |J|^2 \} \quad (10)$$

where m_N is the proton mass, $\eta = m_x/m_N A$, $\xi = \hat{\mathbf{p}}_i \cdot \hat{\mathbf{q}} \geq 0$ (forward scattering) and

$$\sigma_0 = \frac{1}{2\pi} (G_F m_N)^2 \simeq 0.77 \times 10^{-38} \text{ cm}^2 \quad (11)$$

The momentum transfer \mathbf{q} is given by

$$|\mathbf{q}| = q_0 \xi, \quad q_0 = \beta \frac{2m_x c}{1+\eta} \quad (12)$$

Some values of q_0 (forward momentum transfer) for some characteristic values of m_x and representative nuclear systems (light, medium and heavy) are given in Ref. [5]. It is clear from Eq. (12) that the momentum transfer can be sizable for large m_x and heavy nuclei (η small).

Integrating the differential cross section, Eq. (10), with respect to the azimuthal angle we obtain

$$\begin{aligned} d\sigma(u_0, \xi) = & \sigma_0 \left(\frac{m_x}{m_N} \right)^2 \frac{1}{(1+\eta)^2} \{ \{ A^2 [[\beta^2 (f_V^0 - f_V^1 \frac{A-2Z}{A})^2 \right. \\ & + (f_S^0 - f_S^1 \frac{A-2Z}{A})^2] F^2(u_0 \xi^2) - \frac{(\xi \beta)^2}{2} \frac{2\eta+1}{(1+\eta)^2} (f_V^0 - f_V^1 \frac{A-2Z}{A})^2 F^2(u_0 \xi^2)] \\ & + (f_A^0 \Omega_0(0))^2 F_{00}(u_0 \xi^2) + 2f_A^0 f_A^1 \Omega_0(0) \Omega_1(0) F_{01}(u_0 \xi^2) \\ & \left. + (f_A^1 \Omega_1(0))^2 F_{11}(u_0 \xi^2) \} \} 2\xi d\xi \end{aligned} \quad (13)$$

Where

$$F_{\rho\rho'}(u_0 \xi^2) = \sum_{\lambda, \kappa} \frac{\Omega_{\rho}^{(\lambda, \kappa)}(u_0 \xi^2)}{\Omega_{\rho}(0)} \frac{\Omega_{\rho'}^{(\lambda, \kappa)}(u_0 \xi^2)}{\Omega_{\rho'}(0)}, \quad \rho, \rho' = 0, 1 \quad (14)$$

The total cross section $\sigma(u_0, \beta)$, whch has been studied previously (see e.g. [4, 5]), can be cast in the form

$$\begin{aligned} \sigma = & \sigma_0 \left(\frac{m_x}{m_N} \right)^2 \frac{1}{(1+\eta)^2} \{ A^2 [[\beta^2 (f_V^0 - f_V^1 \frac{A-2Z}{A})^2 \right. \\ & + (f_S^0 - f_S^1 \frac{A-2Z}{A})^2] I_0(u_0) - \frac{\beta^2}{2} \frac{2\eta+1}{(1+\eta)^2} (f_V^0 - f_V^1 \frac{A-2Z}{A})^2 I_1(u_0)] \\ & + (f_A^0 \Omega_0(0))^2 I_{00}(u_0) + 2f_A^0 f_A^1 \Omega_0(0) \Omega_1(0) I_{01}(u_0) \\ & \left. + (f_A^1 \Omega_1(0))^2 I_{11}(u_0) \} \end{aligned} \quad (15)$$

The quantities I_{ρ} entering Eq. (13) are defined as

$$I_{\rho}(u_0) = (1+\rho) u_0^{-(1+\rho)} \int_0^{u_0} x^{1+\rho} |F(x)|^2 dx, \quad \rho = 0, 1 \quad (16)$$

where $F(u_0 \xi^2)$ the nuclear form factor and

$$u_0 = q_0^2 b^2 / 2 \quad (17)$$

The integrals $I_{\rho\rho'}$, with $\rho, \rho' = 0, 1$, result by following the standard procedure of the multipole expansion of the $e^{-i\mathbf{q}\cdot\mathbf{r}}$ in Eq. (9). One finds

$$I_{\rho\rho'}(u_0) = 2 \int_0^1 \xi d\xi \sum_{\lambda, \kappa} \frac{\Omega_{\rho}^{(\lambda, \kappa)}(u_0 \xi^2)}{\Omega_{\rho}(0)} \frac{\Omega_{\rho'}^{(\lambda, \kappa)}(u_0 \xi^2)}{\Omega_{\rho'}(0)}, \quad \rho, \rho' = 0, 1 \quad (18)$$

For the evaluation of the differential rate, which is the main subject of the present work, it will be more convenient to use the variables (v, u) instead of the variables (v, ξ) . Thus we get

$$\begin{aligned} d\sigma(u, v) = & \sigma_0 \left(\frac{m_x}{m_N} \right)^2 \frac{1}{(1 + \eta)^2} \left\{ A^2 \left[\left(\frac{v}{c} \right)^2 \left(f_V^0 - f_V^1 \frac{A - 2Z}{A} \right)^2 \right. \right. \\ & + \left(f_S^0 - f_S^1 \frac{A - 2Z}{A} \right)^2 F^2(u) - \frac{1}{(\mu_r b)^2} \frac{2\eta + 1}{(1 + \eta)^2} \left(f_V^0 - f_V^1 \frac{A - 2Z}{A} \right)^2 u F^2(u) \left. \right] \\ & + (f_A^0 \Omega_0(0))^2 F_{00}(u) + 2 f_A^0 f_A^1 \Omega_0(0) \Omega_1(0) F_{01}(u) \\ & \left. + (f_A^1 \Omega_1(0))^2 F_{11}(u) \right\} \frac{du}{2(\mu_r b)^2} \end{aligned} \quad (19)$$

$$u = q^2 b^2 / 2, \quad \mu_r = \frac{m_x}{1 + \eta} \quad (20)$$

where μ_r is the reduced mass and the quantity u is related to the experimentally measurable energy transfer Q via the relations

$$Q = Q_0 u, \quad Q_0 = \frac{1}{A m_N b^2} \quad (21)$$

Let us now assume that the LSP is moving with velocity v_z with respect to the detecting apparatus. Then, the detection rate for a target with mass m is given by

$$R = \frac{dN}{dt} = \frac{\rho(0)}{m} \frac{m}{A m_N} |v_z| \sigma(u, v) \quad (22)$$

where $\rho(0) = 0.3 \text{ GeV/cm}^3$ is the LSP density in our vicinity. This density has to be consistent with the LSP velocity distribution (see next section).

The differential rate can be written as

$$dR = \frac{\rho(0)}{m} \frac{m}{A m_N} |v_z| d\sigma(u, v) \quad (23)$$

where $d\sigma(u, v)$ is given by Eq. (19)

3. CONVOLUTION OF THE EVENT RATE

We have seen that the event rate for LSP-nucleus scattering depends on the relative LSP-target velocity. In this section we will examine the consequences of the Earth's revolution around the sun (the effect of its rotation around its axis will be negligible) i.e. the modulation effect. This can be accomplished by convoluting the rate with the velocity distribution. Such a consistent choice can be a Maxwell distribution [1]

$$f(v') = (\sqrt{\pi} v_0)^{-3} e^{-(v'/v_0)^2} \quad (24)$$

provided that

$$v_0 = \sqrt{(2/3)\langle v^2 \rangle} = 220 \text{ Km/s} \quad (25)$$

For our purposes it is convenient to express the above distribution in the laboratory frame, i.e.

$$f(\mathbf{v}, \mathbf{v}_E) = (\sqrt{\pi}v_0)^{-3} e^{-(\mathbf{v}+\mathbf{v}_E)^2/v_0^2} \quad (26)$$

where \mathbf{v}_E is the velocity of the Earth with respect to the center of the distribution. Choosing a coordinate system in which $\hat{\mathbf{x}}_2$ is the axis of the galaxy, $\hat{\mathbf{x}}_3$ is along the sun's direction of motion (\mathbf{v}_0) and $\hat{\mathbf{x}}_1 = \hat{\mathbf{x}}_2 \times \hat{\mathbf{x}}_3$, we find that the position of the axis of the ecliptic is determined by the angle $\gamma \approx 29.80$ (galactic latitude) and the azimuthal angle $\omega = 186.3^0$ measured on the galactic plane from the $\hat{\mathbf{x}}_3$ axis [5].

Thus, the axis of the ecliptic lies very close to the x_2x_3 plane and the velocity of the Earth is

$$\mathbf{v}_E = \mathbf{v}_0 + \mathbf{v}_1 = \mathbf{v}_0 + v_1 (\sin\alpha \hat{\mathbf{x}}_1 - \cos\alpha \cos\gamma \hat{\mathbf{x}}_2 + \cos\alpha \sin\gamma \hat{\mathbf{x}}_3) \quad (27)$$

Furthermore

$$\mathbf{v}_0 \cdot \mathbf{v}_1 = v_0 v_1 \frac{\cos \alpha}{\sqrt{1 + \cot^2 \gamma \cos^2 \omega}} \approx v_0 v_1 \sin \gamma \cos \alpha \quad (28)$$

where v_0 is the velocity of the sun around the center of the galaxy, v_1 is the speed of the Earth's revolution around the sun, α is the phase of the Earth orbital motion, $\alpha = 2\pi(t - t_1)/T_E$, where t_1 is around second of June and $T_E = 1 \text{ year}$.

The mean value of the differential event rate of Eq. (23), is defined by

$$\left\langle \frac{dR}{du} \right\rangle = \frac{\rho(0)}{m_\chi} \frac{m}{Am_N} \int f(\mathbf{v}, \mathbf{v}_E) |v_z| \frac{d\sigma(u, v)}{du} d^3\mathbf{v} \quad (29)$$

It can be more conveniently expressed as

$$\left\langle \frac{dR}{du} \right\rangle = \frac{\rho(0)}{m_\chi} \frac{m}{Am_N} \sqrt{\langle v^2 \rangle} \left\langle \frac{d\Sigma}{du} \right\rangle \quad (30)$$

where

$$\left\langle \frac{d\Sigma}{du} \right\rangle = \int \frac{|v_z|}{\sqrt{\langle v^2 \rangle}} f(\mathbf{v}, \mathbf{v}_E) \frac{d\sigma(u, v)}{du} d^3\mathbf{v} \quad (31)$$

Thus, taking the polar axis in the direction \mathbf{v}_E , we get

$$\left\langle \frac{d\Sigma}{du} \right\rangle = \frac{4}{\sqrt{6\pi}v_0^4} \int_0^\infty v^3 dv \int_{-1}^1 |\xi| d\xi e^{-(v^2 + v_E^2 + 2vv_E\xi)/v_0^2} \frac{d\sigma(u, v)}{du} \quad (32)$$

or

$$\left\langle \frac{d\Sigma}{du} \right\rangle = \frac{2}{\sqrt{6\pi}v_E^2} \int_0^\infty v dv F_0\left(\frac{2vv_E}{v_0^2}\right) e^{-(v^2 + v_E^2)/v_0^2} \frac{d\sigma(u, v)}{du} \quad (33)$$

with

$$F_0(\chi) = \chi \sinh \chi - \cosh \chi + 1 \quad (34)$$

Introducing the parameter

$$\delta = \frac{2v_1}{v_0} = 0.27, \quad (35)$$

expanding in powers of δ and keeping terms up to linear in it we can write Eq. (33) as

$$\begin{aligned} \left\langle \frac{d\Sigma}{du} \right\rangle = & \sigma_0 \left(\frac{m_x}{m_N} \right)^2 \frac{1}{(1+\eta)^2} \left\{ A^2 \left[[\beta_0^2 (f_V^0 - f_V^1 \frac{A-2Z}{A})^2 \bar{F}_1(u) \right. \right. \\ & + (f_S^0 - f_S^1 \frac{A-2Z}{A})^2] \bar{F}_0(u) - \frac{1}{(\mu_r b)^2} \frac{2\eta+1}{(1+\eta)^2} (f_V^0 - f_V^1 \frac{A-2Z}{A})^2 u \bar{F}_0(u) \left. \right] \\ & + (f_A^0 \Omega_0(0))^2 \bar{F}_{00}(u) + 2f_A^0 f_A^1 \Omega_0(0) \Omega_1(0) \bar{F}_{01}(u) \\ & \left. \left. + (f_A^1 \Omega_1(0))^2 \bar{F}_{11}(u) \right\} a^2 \right\} \end{aligned} \quad (36)$$

with $\beta_0 = v_0/c$ and

$$a = \frac{1}{\sqrt{2} \mu_r b v_0} \quad (37)$$

The quantities $\bar{F}_0, \bar{F}_1, \bar{F}_{00}, \bar{F}_{01}, \bar{F}_{11}$ are obtained from the corresponding form factors via the equations

$$\bar{F}_0(u) = F^2(u) [\Phi_0^{(0)}(a\sqrt{u}) + 0.135 \cos \alpha \Phi_0^{(1)}(a\sqrt{u})] \quad (38)$$

$$\bar{F}_{\rho,\rho'}(u) = F_{\rho,\rho'}(u) [\Phi_0^{(0)}(a\sqrt{u}) + 0.135 \cos \alpha \Phi_0^{(1)}(a\sqrt{u})] \quad (39)$$

$$\bar{F}_1(u) = F^2(u) [\Phi_1^{(0)}(a\sqrt{u}) + 0.135 \cos \alpha \Phi_1^{(1)}(a\sqrt{u})] \quad (40)$$

$$\Phi_k^{(l)}(x) = \frac{2}{\sqrt{6\pi}} \int_x^\infty dy y^{2k-1} (\exp(-y^2)) F_l(2y) \quad (41)$$

with $F_0(\chi)$ given in Eq. (34) and

$$F_1(\chi) = 2 \left[\left(\frac{\chi^2}{4} + 1 \right) \cosh \chi - \chi \sinh \chi - 1 \right] \quad (42)$$

For the cases we considered in this work we find that the quantities $\bar{F}_{\rho,\rho'}(u)$ are almost the same for all isospin channels. We believe this to be a more general result. The value of 0.135 was obtained using $\sin \gamma \approx 0.5$

Combining Eqs. (30), (36) and (38) - (41) we obtain

$$\left\langle \frac{dR}{du} \right\rangle = R^0 t^0 R r_0 [1 + \cos \alpha H(u)] \quad (43)$$

In the above expressions R^0 is the rate obtained in the conventional approach [4] by neglecting the momentum transfer dependence of the differential cross section, i.e. by integrating Eq. (30) after the form factors \bar{F} entering Eq. (36) have been neglected. The parameter t^0 is the additional factor needed when the form factors are included and the total event rate is convoluted with the velocity distribution. $R r_0$ is the relative differential rate, i.e. the differential rate divided by the total rate, in the absence of modulation, i.e.

$$R r_0 = \frac{1}{t^0} \frac{dr^{(0)}}{du} \quad (44)$$

Note that in the above expressions t^0 was defined so that the quantity $R r_0$ is normalized to unity when integrated from u_{min} to infinity. From Eqs. (38) - (41) we

see that if we consider each mode separately the differential modulation amplitude H takes the form

$$H(u) = 0.135 \frac{\Phi_k^{(0)}(a\sqrt{u})}{\Phi_k^{(1)}(a\sqrt{u})} \quad (45)$$

Thus in this case H depends only on u and a . This means that, if we neglect the coherent vector contribution, which, as we have mentioned, is justified, H essentially depends only on the momentum transfer, the reduced mass and the size of the nucleus.

Integrating Eq. (43) we get

$$R = R^0 t^0 [1 + \cos \alpha h(u_0, Q_{min})] \quad (46)$$

where Q_{min} is the energy transfer cutoff imposed by the detector. The effect of folding with LSP velocity on the total rate is taken into account via the quantity t^0 . All other SUSY parameters have been absorbed in R^0 . Strictly speaking the quantity h also depends on the SUSY parameters. It does not depend on them, however, if one considers the scalar, spin etc. modes separately.

Returning to the differential rate it is sometimes convenient, as we will see later, to write it in a slightly different form

$$\left\langle \frac{dR}{du} \right\rangle = R^0 t^0 (Rr0 + \cos \alpha Rr1) \quad (47)$$

$Rr1$ contains the effect of modulation and is given by

$$Rr1 = \frac{1}{t^0} \frac{dr^{(1)}}{du} \quad (48)$$

The meaning of $Rr0$ and $Rr1$ will become more transparent if we consider each mode separately. Thus for the scalar interaction we get $R^0 \rightarrow R_{scalar}^0$ and

$$\frac{dr^{(0)}}{du} = a^2 F^2(u) \Phi_0^{(0)}(a\sqrt{u}) \quad (49)$$

$$\frac{dr^{(1)}}{du} = 0.135 a^2 F^2(u) \Phi_0^{(1)}(a\sqrt{u}) \quad (50)$$

For the spin interaction we get a similar expression except that $R^0 \rightarrow R_{spin}^0$ and $F^2 \rightarrow F_{\rho, \rho'}^2$. Finally for completeness we will consider the less important vector contribution. We get $R^0 \rightarrow R_{vector}^0$ and

$$\frac{dr^{(0)}}{du} = a^2 F^2(u) [\Phi_1^{(0)}(a\sqrt{u}) - \frac{1}{(\mu_r b)^2} \frac{2\eta + 1}{(1 + \eta)^2} \frac{u}{\beta_0^2} \Phi_0^{(0)}(a\sqrt{u})] \quad (51)$$

$$\frac{dr^{(1)}}{du} = 0.135 a^2 F^2(u) [\Phi_1^{(1)}(a\sqrt{u}) - \frac{1}{(\mu_r b)^2} \frac{2\eta + 1}{(1 + \eta)^2} \frac{u}{\beta_0^2} \Phi_0^{(1)}(a\sqrt{u})] \quad (52)$$

We see that, if we consider each mode separately, $Rr0$ and $Rr1$ are independent of all the SUSY parameters except for m_χ . They depend upon the nuclear physics via the relevant form factors.

4. RESULTS AND DISCUSSION

The three basic ingredients of the LSP-nucleus scattering are the input SUSY parameters, a quark model for the nucleon and the structure of the nuclei involved. Experimentally one is interested in the differential rate. In the present work we found it convenient to express it in the manner given by Eq. (43), i.e. in terms of the parameters R^0 , t^0 , $Rr0$ and the convolution amplitude H . The parameter R^0 contains all the information regarding the SUSY model. It has been discussed previously (see e.g Refs. [4, 5]) and it is not the subject of the present work. The other parameters will be discussed below. One is also interested in the total rate (see Eq. (46)). For this, instead of $Rr0$ and H , one needs the convolution parameter h .

The parameter t^0 expresses the modification of the event rate due to its dependence on the velocity of the LSP and the folding with the LSP velocity distribution. The obtained results, which depend on the LSP mass, the nuclear form factors and the detector energy cutoff, Q_{\min} , are presented in Tables Ia and IIa for four nuclear targets of experimental interest.

The obtained results for h , the modulation of the total event rate, are shown in Table Ib for Pb and in Table IIb for some other nuclei of experimental interest. We notice that typically h is quite small, $\leq 5\%$. Quite surprisingly it can become much larger for fairly light LSP and large detector energy cutoff. In other words, in such cases as the cutoff energy increases the modulated amplitude decreases less than the unmodulated one. There seems, therefore, to be a kind of trade off between the total rate and the modulation amplitude. Thus the detector imposed cutoffs may yield a bonus of sizable modulation effect, if the event rate is still detectable.

The quantity which the experiments attempt to measure is the differential rate. In the present work we found it convenient to work with the relative differential event rate with respect to the energy transfer Q , i.e. the differential rate divided by the total rate. Instead of Q we found it convenient to express our results in terms of the dimensionless parameter u introduced above (see Eq. (20)). The parameter u is related to the energy transfer by $Q = Q_0 u$ with Q_0 given by Eq. (21).

We focused our attention on the modulation amplitude which is described either by the parameter H (see Eq. (43)) or by $Rr1$ (see eq.(48)). $Rr1$ and H are independent of the SUSY parameters and the structure of the nucleon. $Rr1$ mildly depends on the nuclear structure, i.e. it depends on the reduced mass of the system, the nuclear form factor and the lower energy cutoff imposed by the detectors. H is even independent of the nuclear form factor, but somehow it depends on the size of the nucleus.

Summarizing our results we can say the following :

1. The nucleus $^{82}Pb^{207}$ [4, 5].

In this case $Q_0 = 40$ KeV. We considered both the coherent and the spin contribution for

$$m_\chi = 30, 50, 80, 100, 125, 250, 500 \text{ GeV} \text{ and } Q_{\min} = 0, 20, 40 \text{ KeV}$$

employing the harmonic oscillator form factors of Ref. [22]. Our results are presented in Fig. 1(a)-(j). Since the parameter H is independent of Q_{min} , it is only shown for $Q_{min} = 0$. We see that H rises with u and for the same u it decreases with the LSP mass. It can become as large as 25 % for light LSP (see Fig. 1(c)). We notice, however, that the event rate drops sharply after $u = 0.4$, i.e. $Q = 16$ KeV. Thus, the most favored region is around $u = 0.2$ or $Q = 8$ KeV (see Fig. 1(b)). We also see that H is negative at small u and becomes positive as u increases. Notice, however, that the event rate is large at low u (see Fig. 1(a)). Hence we have cancellations in the total modulation amplitude. The analogous results for $Q_{min} = 20$ KeV are shown in Figs. 1(d)-(e). The latter results are shifted compared to the previous ones by $\Delta u = 0.125$ but they appear otherwise similar. This is misleading since it is the result of the normalization adopted (the area under the curves of Figs 1(a) and 1(d) is normalized to unity). Notice that the absolute rates are down about a factor of 3 from those at $Q_{min} = 0$. We see from Table Ia that the total event rates are very much suppressed for $Q_{min} = 40$ KeV. Thus if such cutoffs are required by the detector, the process is unobservable. We also present results for the spin contribution for the isospin (11) channel in Figs. 1(f)-(g) for $Q_{min} = 0$. Our results for $Q_{min} = 20$ KeV compared to those of $Q_{min} = 0$ show a similar trend as those of Figs. 1(d)-(e) when compared to those of Figs. 1(a)-(b). The other isospin channels show behavior similar to the (11) channel [5]. Thus we can say in general that the differential rate due to the spin contribution falls quite a bit slower compared to the coherent rate as a function of u . We also know that the total rate shows a similar trend with respect to u_0 [5]. Furthermore, the quantity $Rr1$ is a bit broader, which means that the modulation effect is somewhat favored in the spin contribution since a broader energy window around the maximum can be selected. For purposes of comparison, we present in Figs. 1(h)-(j) the analogous results for $Q_{min} = 0$ obtained for the less important coherent vector contribution. We see that, in addition to the couplings, the LSP velocity distribution favors the vector contribution, but this, of course, is not enough to overcome the suppression factor β_0^2 (see Eq. (36)) due to the Majorana nature of the LSP.

2. The nucleus $^{53}I^{127}$.

This nucleus is of great experimental interest [21] due to the advantages of the NaI detector. In this case $Q_0 = 60$ KeV. We show results for the coherent scalar interaction employing the harmonic oscillator form factors of Ref. [22] for

$$m_\chi = 30, 50, 80, 100, 125, 250 \text{ GeV and } Q_{min} = 0, 45 \text{ KeV}$$

Even though for $Q_{min} = 45$ KeV the total rate is suppressed (see Table IIa), for the benefit of the experimentalists we will present the corresponding results for the differential rate. We do not show the differential rate for $m_\chi = 10$ since falls off too fast as a function of u . So there is no advantage in going to an energy window. Our results are shown in Figs. 2(a)-(c) and Figs. 2(d)-(e) for $Q_{min} = 0, 45$ KeV respectively. Results for $Q_{min} = 0$ KeV are also shown in Figs. 2(g)-(h) in the case of the spin contribution for the isospin (11) channel. The other channels show a similar behavior. The spin form factors were taken from Ref. [7].

3. The nucleus $^{11}Na^{23}$.

This nucleus is a part of the same detector as in the previous one. Here $Q_0 = 630$ KeV. Even though for this light nucleus the spin contribution may be relatively more important compared to the coherent one, we only considered in this work the coherent contribution in a fashion analogous to the Al case discussed below. The parameters t^0 and h are shown in Tables IIa, IIb respectively. In this case the detector energy cutoff is 8 – 16 KeV. Our results for the differential rate for zero energy cut off are similar to those for Al listed below. For $Q_{min} = 16$ KeV they are shown in Figs. 3(a)-(b). We see that in all cases the differential rate falls off real fast as a function of u . This is not surprising since for such a light system the momentum transferred to the nucleus cannot be large.

4. The nucleus $^{13}Al^{27}$.

A detector with this nucleus has the advantage of very low energy threshold $Q_{min} = 0.5$ KeV. In this case $Q_0 = 480$ KeV. Again only the coherent scalar contribution was considered. Both harmonic oscillator and Woods-Saxon form factors were tried. The difference between them was small. The results presented were obtained with the Woods-Saxon form factors with $c = 3.07$ and $a_0 = 0.519$ fm [23]. The parameters t^0 and h for various LSP masses and cutoffs are given in Tables IIa and IIb respectively. In our plots we considered the values of $m_\chi = 10, 20, 30, 50$ GeV. For larger masses the results remain unchanged. For $Q_{min} = 0.5$ KeV our results for the differential rate are shown in Figs. 4(a)-(c).

4. CONCLUSIONS

Detectable rates for the LSP-nucleus scattering for some choices in the allowed SUSY parameter space are possible [5]. Similar results have been obtained in the form of scatter-plots by Arnowitt and Nath[18] and more will appear elsewhere [20]. Since, anyway, the event rate is indeed very low, one should try to exploit the modulation effect, i.e. the dependence of the event rate on the motion of the Earth.

In the present work, by convoluting the event rate with the LSP velocity distribution we were able to obtain the annual modulation effect, both for the coherent as well as the spin contribution. We were not concerned with the diurnal modulation since it is undetectable. This was done both in the total rate as well as in the differential rate with respect to the energy transferred to the nucleus. For the total rate we found it convenient to write our formalism in terms of three factors (see Eq. (45)). The first one, R^0 , depends on all the relevant SUSY parameters. It represents the total event rate, when the velocity dependence of the cross-section and the convolution are neglected. The second, t^0 , is the modification of the event rate due to the velocity dependence of the cross-section and the procedure of folding with the LSP velocity. The third is the modulation amplitude h . If one considers separately each mode (scalar, spin, vector coherent etc.) t^0 and h depend only on

the LSP mass, the nuclear form factors and Q_{min} . The parameter t^0 for various LSP masses and a number of nuclear systems as a function of various detector energy cutoffs is shown in Tables Ia, IIa. The total modulation amplitude h is shown in Tables Ib, IIb. We see that it is possible to have a modulation effect which is larger than the typical value, $h \leq 5\%$, but in those cases when the total rate is suppressed, e.g. for relatively small LSP mass and large Q_{min} . So detectors with large cutoffs should not be offhand considered to be disadvantaged provided that the total event rate is detectable.

In the case of the differential rate, in addition to the factors t^0 and h mentioned above we needed two more factors (see Eq. (43)). The relative differential rate $Rr0$, i.e. the differential rate divided by the total rate, and the differential modulation amplitude H . If one considers separately each mode, H depends only on the reduced mass and the size of the nucleus. The differential modulated rate $Rr1$ depends in addition on the nuclear form factors. It is negative at small momentum transfer and becomes positive as the momentum transfer increases. As a result, h is always less than 5% [5] and tends to decrease in the case of heavier nuclei. This happens because in the case of $Q_{min} = 0$, contributions from different regions of the momentum transfer tend to cancel.

Our main result is that the differential modulation amplitude H can become quite large as the momentum transfer increases (see Figs. 1(c), 2(c), and 4(c)). Our results are very encouraging. Whether this nice feature, however, can be fully exploited by the experimentalists will depend on whether they can exploit the energy windows around the maximum of $Rr1$ shown in Figs. 1(b), (e), (g), 2(b), 2(e), 3(b) and 4(b). The vector coherent contribution, see Figs. 1(h)-(j), shows even better features, but unfortunately it cannot be utilized, since the total rate R^0 associated with it is suppressed due to the Majorana nature of the LSP.

In any event we found many circumstances such that the modulation effect, both in the total as well as in the differential event rate, may aid the experimentalists in discriminating against background.

Acknowledgements: The author would like to acknowledge partial support of this work by ΠΙΕΝΕΔ 1895/95 of the Greek Secretariat for research, TMR Nos ERB FMAX-CT96-0090 and ERBCHRXCT93-0323 of the European Union and the Bartol Research Foundation where most of the work was done. He would like also to thank Drs S. Pittel and Q. Shafi for their hospitality and useful discussions. Special thanks to Dr T. S. Kosmas for his help in preparing the manuscript.

References

- [1] For a recent review see e.g. G. Jungman *et al.*, Phys. Rep. **267**, 195 (1996).
- [2] G.F. Smoot *et al.*, (COBE data), Astrophys. J. **396**, L1 (1992).
- [3] D.P. Bennett *et al.*, (MACHO collaboration), A binary lensing event toward the LMC: Observations and Dark Matter implications, Proc. 5th Annual Maryland Conference, edited by S. Holt (1995);
C. Alcock *et al.*, (MACHO collaboration), Phys. Rev. Lett. **74**, 2967 (1995).

- [4] J.D. Vergados, J. of Phys. **G 22**, 253 (1996).
- [5] T.S. Kosmas and J.D. Vergados, Phys. Rev. **D 55**, 1752 (1997).
- [6] M. Drees and M.M. Nojiri, Phys. Rev. **D 48**, 3843 (1993); Phys. Rev. **D 47**, 4226 (1993).
- [7] M.T. Ressell *et al.*, Phys. Rev. **D 48**, 5519 (1993); M.T. Ressel and D.J. Dean, hep-ph/9702290.
- [8] V.I. Dimitrov, J. Engel and S. Pittel, Phys. Rev. **D 51**, R291 (1995).
- [9] J. Engel, Phys. Lett. **B 264**, 114 (1991).
- [10] M.A. Nikolaev and H.V. Klapdor-Kleingrothaus, Z. Phys. **A 345**, 373 (1993); Phys. Lett **329 B**, 5 (1993); Phys. Rev. **D 50**, 7128 (1995).
- [11] A.K. Drukier *et al.*, Phys. Rev. **D 33**, 12 (1986);
J.I. Collar *et al.*, Phys. Lett **B 275**, 181 (1992).
- [12] P.F. Smith and J.D. Lewin, Phys. Rep. **187**, 203 (1990).
- [13] J.R. Primack, D. Seckel and B. Sadoulet, Ann. Rev. Nucl. Part. Sci. **38**, 751 (1988);
F. von Feilitzsch, Detectors for Dark Matter Interactions Operated at Low Temperatures, Int. Workshop on Neutrino Telescopes, Venezia Feb. 13-15, 1990 (ed. Milla Baldo Ceolin) p. 257.
- [14] R. Bernabei *et al.*, Phys. Lett. **B 389**, 757 (1996).
- [15] M.W. Goodman and E. Witten, Phys. Rev. **D 31**, 3059 (1985);
K. Griest, Phys. Rev. Lett **62**, 666 (1988); Phys. Rev. **D 38**, 2357 (1988) ; **D 39**, 3802 (1989);
J. Ellis, and R.A. Flores, Phys. Lett. **B 263**, 259 (1991); Phys. Lett **B 300**, 175 (1993); Nucl. Phys. **B 400**, 25 (1993);
J. Ellis and L. Roszkowski, Phys. Lett. **B 283**, 252 (1992).
- [16] A. Bottino *et al.*, Mod. Phys. Lett. **A 7**, 733 (1992); Phys. Lett. **B 265**, 57 (1991); Phys. Lett **B 402**, 113 (1997); hep-ph / 9709222; hep-ph /9710296;
J. Edsjo and P Gondolo, Phys. Rev. **D 56**, 1789 (1997);
Z. Berezinsky *et al.*, Astroparticle Phys. **5**, 1 (1996);
V.A. Bednyakov, H.V. Klapdor-Kleingrothaus and S.G. Kovalenko, Phys. Lett. **B 329**, 5 (1994).
- [17] G.L. Kane *et al.*, Phys. Rev. **D 49**, 6173 (1994);
D.J. Castaño, E.J. Piard and P. Ramond, Phys. Rev. **D 49**, 4882 (1994);
D.J. Castaño, Private Communication;
A.H. Chamseddine, R. Arnowitt and P. Nath, Phys. Rev. Lett. **49**, 970 (1982);
P. Nath, R. Arnowitt and A.H. Chamseddine, Nucl. Phys. **B 227**, 121 (1983);
R. Arnowitt and P. Nath, Mod. Phys. Lett. **10**, 1215 (1995);
R. Arnowitt and P. Nath, Phys. Rev. Lett. **74**, 4952 (1995);
R. Arnowitt and P. Nath, Phys. Rev. **D 54**, 2394 (1996).
- [18] L. Arnowitt, Dark matter predictions in non-universal soft breaking masses, NANP-97, Int. Workshop on Non-accelerator New Physics, Dubna, July 7-11, to appear in the proceedings; R. Arnowitt and P. Nath, hep-ph/9701301;
S.K. Soni and H.A. Weldon, Phys. Lett. **B 126**, 215 (1983);

V.S. Kapunovsky and J. Louis, Phys. Lett. **B 306**, 268 (1993);
 M. Drees, Phys. Lett **B 181**, 279 (1986);
 P. Nath and R. Arnowitt, Phys. Rev. **D 39**, 279 (1989);
 J.S. Hagelin and S. Kelly, Nucl. Phys. **B 342**, 95 (1990);
 Y. Kamamura, H. Murayama and M. Yamaguchi, Phys. Lett. **B 324**, 52 (1994);
 S. Dimopoulos and H. Georgi, Nucl. Phys. **B 206**, 387 (1981).

[19] T.S. Kosmas and J.D. Vergados, Searching for cold dark matter: a case of coexistence of supersymmetry and nuclear physics, NANP-97, Int. workshop on non-accelerator new physics, Dubna, July 7-11, to appear in the proceedings.

[20] A. Wodecki, T.S. Kosmas and J.D. Vergados, in preparation.

[21] R. Bernabei et al. , Strategies to search for WIMP annual modulation signature with large-mass low radioactivity NaI(Ti) set up, ROM2F-97-33 preprint(*astro-ph/9710290*);
 R. Bernabei et al., Phys. Lett. **B 389**, 757 (1996).

[22] T.S. Kosmas and J.D. Vergados, Nucl. Phys. **A 510**, 64 (1990).

[23] R. M. Lombard et al., Nucl. Phys. **101**, 601 (1967).

Figure Captions:

Fig. 1: The relative differential event rate $Rr0$ and the amplitudes for modulation $Rr1$ and H vs u for the target $^{82}Pb^{207}$ (for the definitions see text). The curves shown correspond to LSP masses as follows:

i) Thick solid line $\iff m_\chi = 30$ GeV. ii) Solid line $\iff m_\chi = 50$ GeV. iii) Dotted line $\iff m_\chi = 80$ GeV. iv) Dashed line $\iff m_\chi = 100$ GeV. v) Intermediate dashed line $\iff m_\chi = 125$ GeV. vi) Fine solid line $\iff m_\chi = 250$ GeV. vii) Long dashed line $\iff m_\chi = 500$ GeV. If some curves of the above list seem to have been omitted, it is understood that they fall on top of vi). Note that, due to our normalization of $Rr0$, the area under the corresponding curve is unity.

- (a) $Rr0$ for the scalar contribution and $Q_{min} = 0$.
- (b) The amplitude $Rr1$ for the scalar contribution and $Q_{min} = 0$.
- (c) The modulation amplitude H , i.e. the ratio of $Rr1$ divided by $Rr0$ for $Q_{min} = 0$.
- (d) The same as in (a) for $Q_{min} = 20$ KeV.
- (e) The same as in (b) for $Q_{min} = 20$ KeV.
- (f) The same as in (a) for the spin contribution in the isospin (11) channel. For the other isospin channels the results are similar.
- (g) The same as in (b) for the spin contribution in the (11) channel.
- (h) The same as in (a) for the vector coherent contribution.
- (i) The same as in (b) for the vector coherent contribution.
- (j) The same as in (c) for the vector coherent contribution.

Fig. 2: The same as in Fig. 1 for the target $^{53}I^{127}$.

- (a) $Rr0$ for $Q_{min} = 0$.
- (b) $Rr1$ for $Q_{min} = 0$.
- (c) H for $Q_{min} = 0$.
- (d) The same as (a) for $Q_{min} = 45$ KeV.
- (e) The same as (b) for $Q_{min} = 45$ KeV. The style of the curves is the same as in Fig. 1.

Fig. 3: The same as in Fig. 1 for the target $^{13}Na^{23}$. The curves shown correspond to LSP masses as follows:

i) Dotted line $\iff m_\chi = 10$ GeV. ii) Dashed line $\iff m_\chi = 20$ GeV. iii) Long dashed line $\iff m_\chi = 30$ GeV. iv) Fine solid line $\iff m_\chi = 50$ GeV.

For LSP masses heavier than 50 GeV the curves cannot be distinguished from iv).

- (a) $Rr0$ for $Q_{min} = 16$ KeV.
- (b) $Rr1$ for $Q_{min} = 16$ KeV.

Fig. 4: The same as in Fig. 1 for the target $^{13}Al^{27}$ and $Q_{min} = 0.5$ KeV. (a), (b), and (c) refer to $Rr0$, $Rr1$ and H respectively. The style of the curves is the same as in Fig. 3.

TABLE Ia. The quantity t^0 for the target $^{82}Pb^{207}$. t^0 takes into account the velocity dependence of the event rate and the folding with the LSP velocity distribution. It is computed for various LSP masses in the allowed SUSY parameter space. The scalar, the vector coherent ($k=1$) as well as the spin contributions are included. In the latter (11),(01) and (11) indicate the possible isospin channels.

		LSP mass in GeV						
Mode	$Q_{min}(KeV)$	30	50	80	100	125	250	500
Scalar	0	1.23	0.728	0.413	0.316	0.246	0.123	0.0761
	20	0.404	0.331	0.209	0.164	0.129	0.0668	0.0468
	40	0	2×10^{-4}	5×10^{-4}	7×10^{-4}	6×10^{-4}	5×10^{-4}	4×10^{-4}
Vector	0	3.349	1.735	0.902	0.671	0.509	0.248	0.151
Spin (11)	0	1.57	1.298	0.949	0.793	0.661	0.394	0.266
Spin (11)	20	0.082	0.512	0.367	0.344	0.312	0.216	0.155
Spin (00)	0	1.45	1.13	0.793	0.655	0.542	0.318	0.213
Spin (01)	0	1.51	1.21	0.866	0.719	0.597	0.353	0.237

TABLE Ib. The same as in Table Ia for the modulation amplitude h .

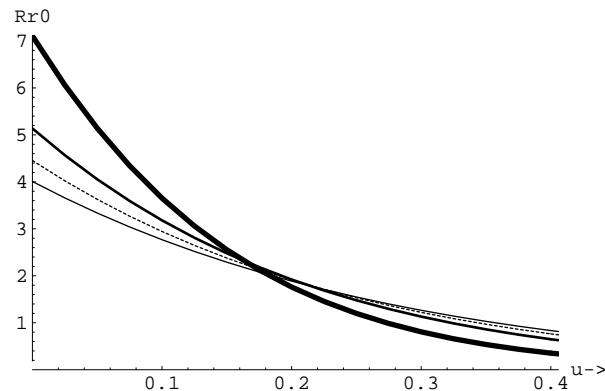
		LSP mass in GeV						
Mode	$Q_{min}(KeV)$	30	50	80	100	125	250	500
Scalar	0	0.0295	0.0151	0.0054	0.0022	-0.0001	-0.0005	-0.0059
	20	0.1543	0.0774	0.0401	0.0292	0.0211	0.0070	0.0013
	40	0.2525	0.1598	0.0991	0.0784	0.0620	0.0314	0.0177
Vector	0	0.0543	0.0621	0.0571	0.0560	0.0553	0.0545	0.0543
Spin (11)	0	0.0460	0.0307	0.9266	0.0219	0.0184	0.0113	0.0066
Spin (11)	20	0.1659	0.0926	0.0549	0.0444	0.0371	0.0234	0.0151
Spin (00)	0	0.0421	0.0349	0.0238	0.0195	0.0163	0.0100	0.0056
Spin (01)	0	0.0440	0.0369	0.0252	0.0207	0.0174	0.0107	0.0061

TABLE IIa. The quantity t^0 for the experimentally interesting targets $^{53}I^{127,11}Na^{23}$ and $^{13}Al^{27}$ (for definitions see Table Ia).

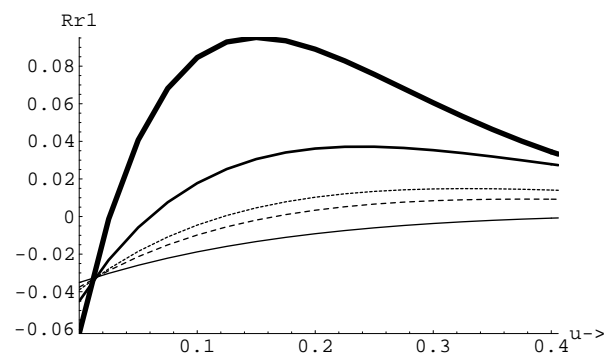
Target	$Q_{min}(KeV)$	LSP mass in GeV						
		10	20	30	50	80	100	125
I Scalar	0	2.16		1.50	1.04	0.689	0.566	0.469
	20	0.0		0.089	0.170	0.162	0.144	0.127
	45	0.0		0.0014	0.0124	0.0198	0.0201	0.0193
Spin (11)	0	2.13		1.40	0.960	0.651	0.553	0.473
	20	0.0		0.075	0.153	0.167	0.164	0.158
	45	0.0		0.0018	0.0288	0.0483	0.0587	0.0674
Na Scalar	0	2.33	2.32	2.31	2.30	2.30	2.30	2.30
	8	0.454	1.19	1.49	1.69	1.69	1.69	1.69
	16	0.064	0.570	0.907	1.19	1.19	1.19	1.19
Al Scalar	0	2.32	2.31	2.30	2.29	2.29	2.29	2.29
	0.5	2.11	2.22	2.24	2.25	2.25	2.25	2.25

TABLE IIb. The same as in Table IIa for the modulation amplitude h .

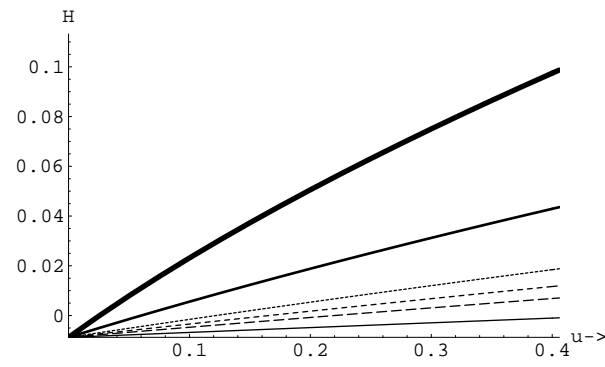
Target	$Q_{min}(KeV)$	LSP mass in GeV						
		10	20	30	50	80	100	125
I Scalar	0	0.0508		.0361	0.0241	0.0139	0.0102	0.0072
	20	0.0		0.1298	0.0734	0.0426	0.0331	0.0258
	45	0.0		0.2194	0.1294	0.0740	0.0588	0.0474
Spin (11)	0	0.0501		0.0344	0.0241	0.0180	0.0166	0.0157
	20	0.0		0.1309	0.0793	0.0568	0.0512	0.0471
	45	0.0		0.2215	0.1402	0.1018	0.0910	0.0809
Na Scalar	0	0.0540	0.0539	0.0537	0.0535	0.0535	0.0535	0.0535
	8	0.1334	0.0906	0.0793	0.0715	0.0715	0.0715	0.0715
	16	0.2039	0.1237	0.1030	0.0911	0.0911	0.0911	0.0911
Al Scalar	0	0.0538	0.0538	0.0596	0.0534	0.0534	0.0534	0.0534
	0.5	0.0598	0.0563	0.0553	0.0545	0.0545	0.0545	0.0545



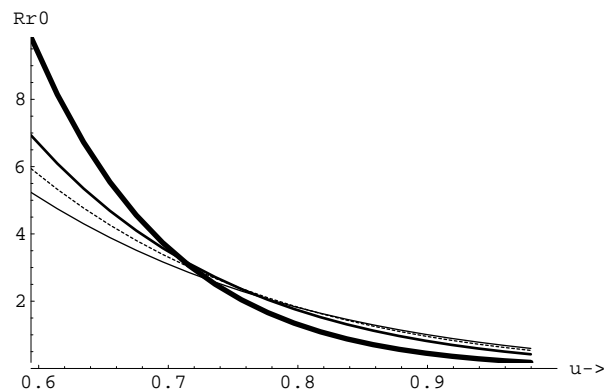
(a)



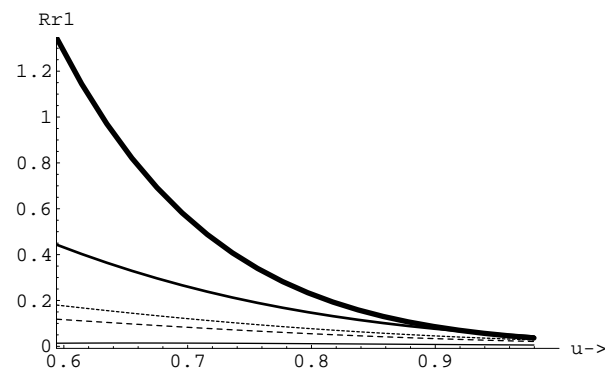
(b)



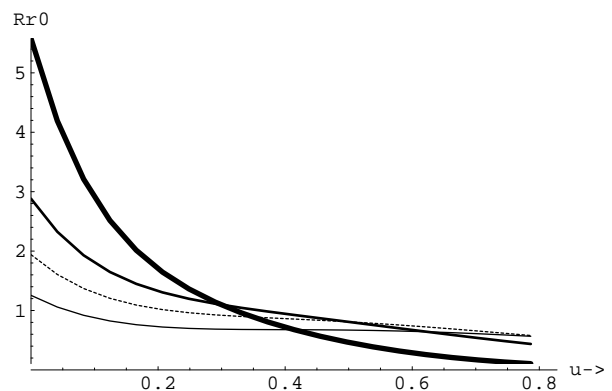
(c)



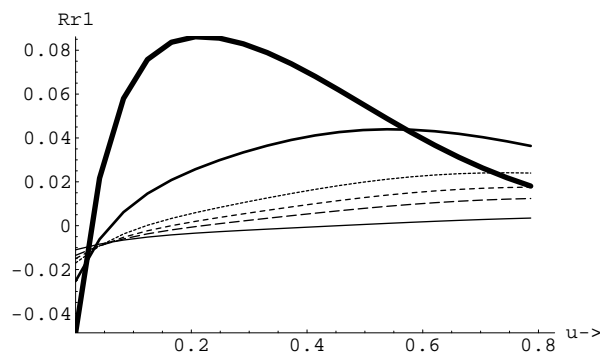
(d)



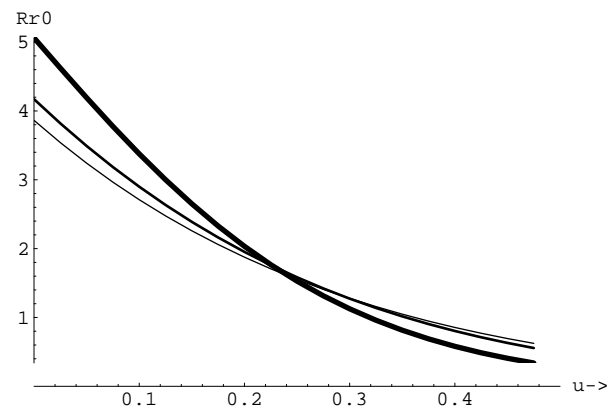
(e)



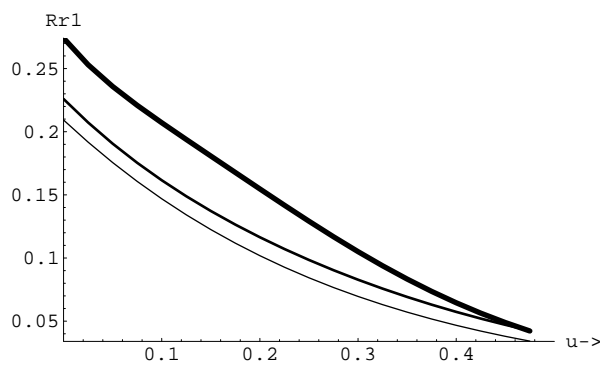
(f)



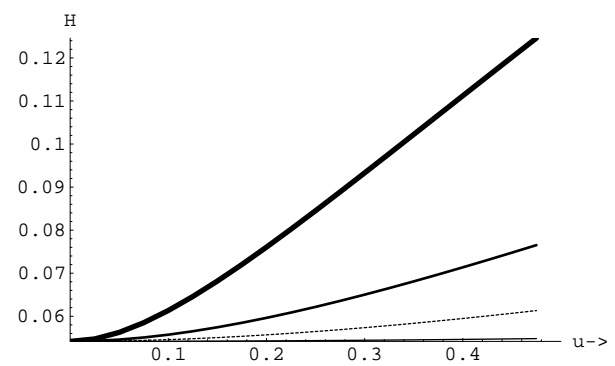
(g)



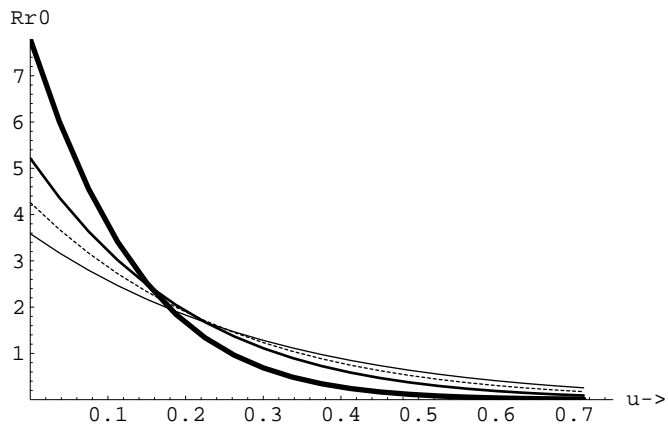
(h)



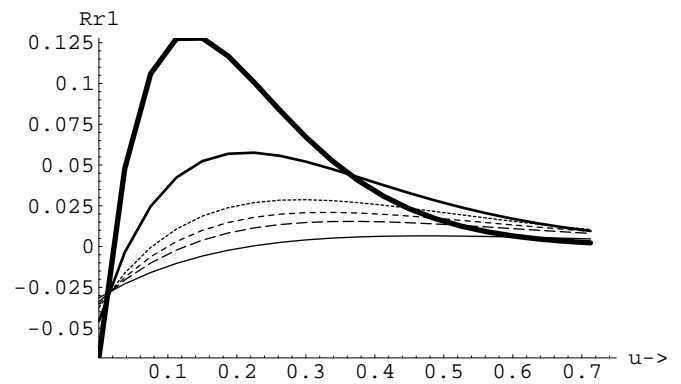
(i)



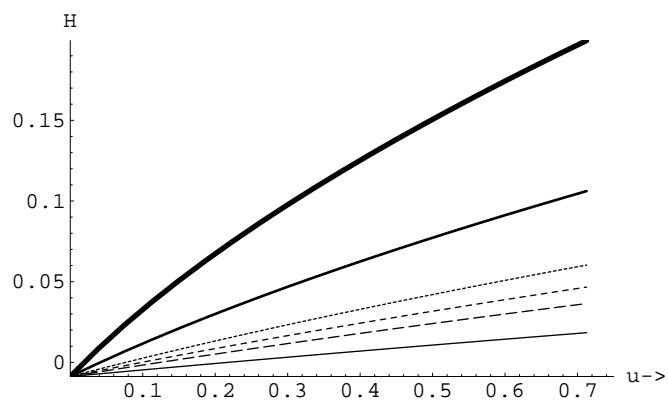
(j)



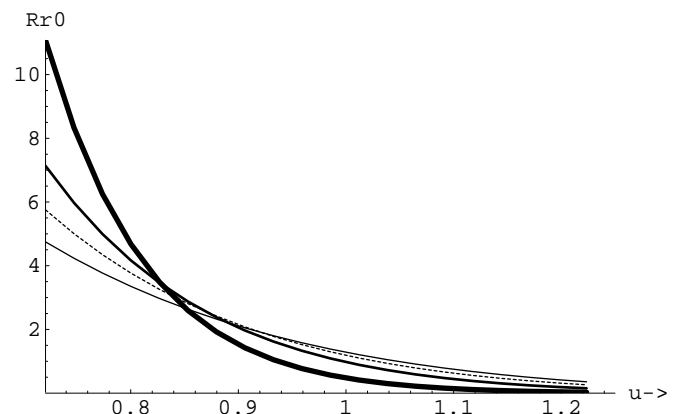
(a)



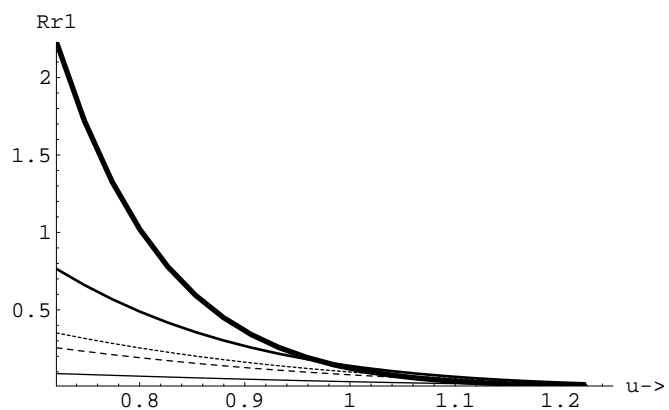
(b)



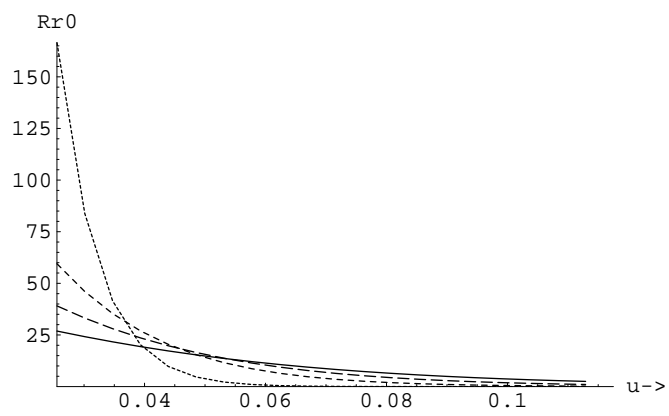
(c)



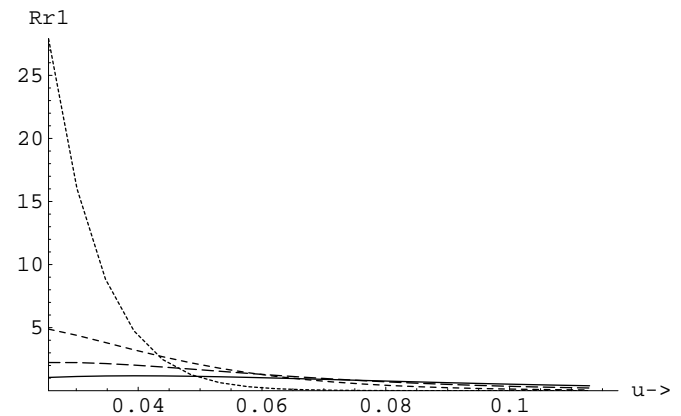
(d)



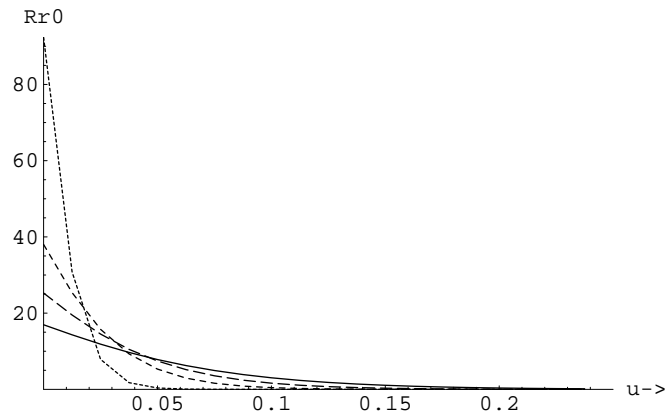
(e)



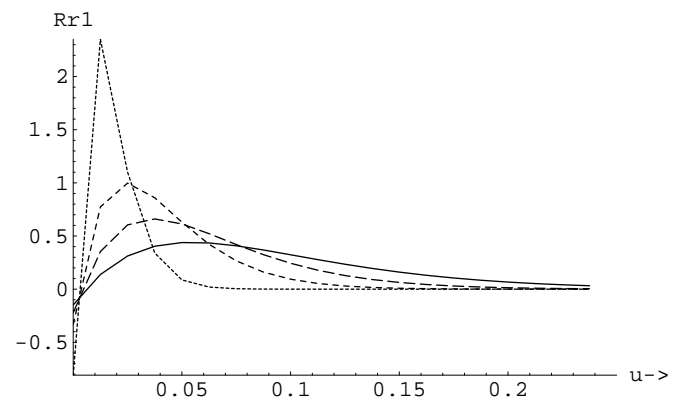
(a)



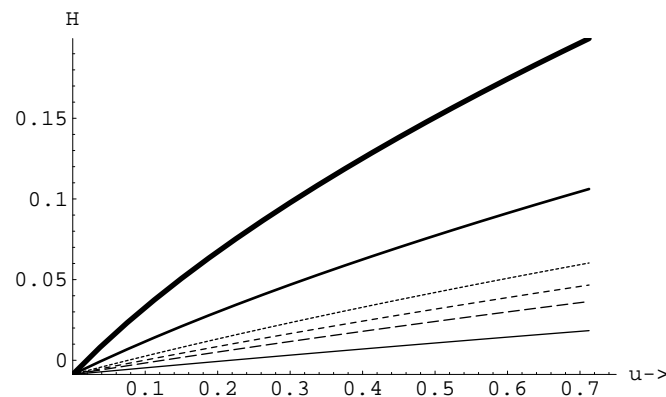
(b)



(a)



(b)



(c)